Modern Research in Catalysis, 2019, 8, 11-23
https://www.scirp.org/journal/mrc
ISSN Online: 2168-4499
ISSN Print: 2168-4480

Nanosized Au Catalysts Supported on $Mg(OH)_2$-CeO_2 for Preferential Oxidation of CO in Hydrogen Stream

Yu-Wen Chen[1*], Anton S. Brichkov[2], Vladmir V. Kozik[2]

[1]Department of Chemical and Materials Engineering, National Central University, Taoyuan, Chinese Taipei
[2]Department of Chemistry, Tomsk State University, Tomsk, Russia
Email: *ywchen@cc.ncu.edu.tw

How to cite this paper: Chen, Y.-W., Brichkov, A.S. and Kozik, V.V. (2019) Nanosized Au Catalysts Supported on $Mg(OH)_2$-CeO_2 for Preferential Oxidation of CO in Hydrogen Stream *Modern Research in Catalysis*, **8**, 11-23.
https://doi.org/10.4236/mrc.2019.82002

Received: April 5, 2019
Accepted: April 27, 2019
Published: April 30, 2019

Abstract

Preferential oxidation of carbon monoxide in the presence of hydrogen (PROX) is a promising method to remove CO from a hydrogen-containing gas mixture. Nanosized gold catalyst supported on CeO_2 and modified with $Mg(OH)_2$ was used for preferential oxidation of carbon monoxide in hydrogen-rich stream in this study. $Mg(OH)_2$ was added on CeO_2 by incipient-wetness impregnation. Au was loaded on $Mg(OH)_2$-CeO_2 by deposition-precipitation method. PROX reaction was carried out in a continuous flow, fixed bed reactor. CO/O_2 feed ratio was fixed at 1 to magnify the difference of various catalysts. The catalysts were characterized by N_2 sorption, TEM, HR-TEM and XPS. $Mg(OH)_2$ formed a thin layer on the surface of CeO_2. CeO_2 was in the crystalline phase and $Mg(OH)_2$ was amorphous. Au particles were homogeneously dispersed on the support with a size of 2 - 5 nm. Using CeO_2 as a support could increase the dispersion of $Mg(OH)_2$ and thus increase the interaction between Au and $Mg(OH)_2$. Adding $Mg(OH)_2$ on Au/CeO_2 could suppress H_2 oxidation and therefore increase CO oxidation activity.

Keywords

Gold, CO Oxidation, Hydrogen Energy, Cerium Oxide

1. Introduction

The hydrogen containing mixture used to feed portable power units based on proton-exchange membrane fuel cells (PEMFCs) is obtained through the conversion of hydrocarbon with steam reforming. These mixtures usually contain 0.5 - 2 vol. % of CO, 15 - 25 vol. % of CO_2, and 5 - 10 vol. % of water vapor. Because CO is a poison to PEMFC anodes, its concentration should be reduced to a level of less than 10 ppm. The preferential oxidation of carbon monoxide in the presence of hydrogen (PROX) is a promising method for removing CO from hydrogen-containing gas mixture [1]-[10]. It contains two reactions:

$$2CO = O_2 = 2CO_2 \quad (1)$$

$$2H_2 = O_2 = 2H_2O \quad (2)$$

Reaction (2) of hydrogen oxidation leads to a loss of fuel for a PEMFC and lowers the efficiency of process; it is therefore desirable to suppress this reaction. Supported gold nanoparticles are promising catalysts for the preferential oxidation of CO. The catalysts which are able to selectively oxidize CO in the presence of excess H_2 should possess high CO oxidation activity as well as inhibit oxidation of H_2 at the temperature region of the PEM fuel cells (80˚C - 100˚C) [1] [2] [3] [4] [5].

The promotional effect of oxidation of CO in the existence of hydrogen has been reported by many researchers [11] [12]. CO adsorption and oxidation on Au/MgO have been studied extensively [11]-[17]. Cunningham *et al.* [11] suggested that the CO was directly reacted with hydroxyl radicals located at the interface of gold and $Mg(OH)_2$. These active hydroxyl radicals on the $Mg(OH)_2$ surface strongly interacted with the gold. Tompos *et al.* [14] reported that Pb, Sm and V-promoted Au/MgO catalysts were very active and selective for CO oxidation in the presence of hydrogen. However, high Au metal loading (>2.8 wt%) was used in their study. In addition, commercial MgO was used as a support and it had low surface area.

Au supported on MgO (001) was studied using various DFT approaches with either cluster or periodic geometries [15]. The vacancy defects were associated with the surfaces of Au nanoparticles embedded in MgO, indicating that Au atoms intend to attach to the defect sites. Cunningham *et al.* [11] used Al_2O_3 as a support for MgO and Au. However, Al_2O_3 is not good a support for Au, since its isoelectric point is too low and it lacks oxygen vacancy.

MgO has low surface area. If one can prepare MgO thin film with many defect sites on the surface of CeO_2, it would have high surface area of MgO and many defect sites. One can deposit Au on $Mg(OH)_2$-CeO_2 which has the similar properties as Au/MgO. In a previous study, one of the authors [18] has reported that Au/MgO_x-TiO_2 demonstrated high PROX performance. However, Au supported on $Mg(OH)_2$-CeO_2 has never been reported in the literature.

In this study, Au catalysts supported on $Mg(OH)_2$-CeO_2 with various $Mg(OH)_2$ contents were prepared. Various techniques were used to characterize the catalysts. The aim of this study was to investigate the effects of Mg content in Au/$Mg(OH)_2$-CeO_2 catalyst on the activity and selectivity of oxygen reacting with CO in PROX reaction.

2. Experimental

2.1. Catalys Preparation

A series of $Mg(OH)_2$-CeO_2 with various $Mg(OH)_2$ contents were prepared by co-precipitation method [1]-[10] using magnesium nitrate and cerium nitrate as the starting materials. The catalyst was dried overnight in air at 80˚C for 8 h, and then calcined at 550˚C for 4 h in air. Deposition-precipitation method (DP) was used in this study to deposit gold on the support. The detailed preparation method has been described in previous paper [18]. An aqueous solution of $HAuCl_4$ (2.55×10^{-3} M) was slowly added into the solution containing support under vigorous stirring at a temperature 65˚C. NH_4OH was used to adjust the pH value of the solution to 7. After aging for 2 h, the sample was filtered and the filtration cake was washed until no chloride ions were detected. Finally, the sample was dried overnight at 80˚C, and was calcined at 180˚C for 4 h. This temperature was high enough to reduce Au^3 = cation and low enough to prevent Au from sintering. The nominal loading of Au was 1 wt%. The sample was denoted as $Au/Mg(OH)_2$-$CeO_2(x)$ where x is the atomic ratio of Mg/(Mg + Ce).

2.2. Catalysts Characterization

The catalysts were characterized with ICP-MS, N_2-sorption, transmission electron micros copy (TEM), high resolution transmission electron microscopy (HR-TEM), X-ray diffraction (XRD), and X-ray Spectroscopy (XPS). The characterization technique has been described in the previous paper [18]. The real Au contents of the catalysts were measured by ICP-MS.

The surface area of the samples was measured using a Micromeritics ASAP 2010 by Brunauer-Emmett-Teller (BET) method in the range $P/P_0 = 0.05$ - 0.3. Prior to the experiments, the sample was treated at 120˚C for 8 h at the vacuum pressure below 1×10^{-5} torr.

XRD analysis was performed using a Siemens D500 powder diffractometer using Cu $K_{\alpha 1}$ radiation (0.15405 nm) at a voltage and current of 40 kV and 40 mA, respectively. The sample was scanned over the range of $2\theta = 20^\circ$ - 70˚ at a rate of 0.05˚/min.

The catalysts were characterized by TEM on a JEM-2000 EX II operated at 120 kV and HRTEM on a JEOL JEM-2010 operated at 160 kV. A small amount of sample was placed into the sample tube filled with a 95% ethanol solution. After agitating under ultrasonic environment for 3 h, one drop of the sample was dipped on a carbon-coated copper mesh (300#) (Ted Pella Inc., CA, USA), then dried in vacuum overnight. Images were recorded digitally with a Gatan slow scan camera (GIF).

XPS analysis was carried out with a Thermo VG Scientific Sigma Prob spectrometer. The XPS spectra were collected using Al K_α radiation at a voltage and current of 20 kV and 30 mA, respectively. The spectrometer was operated at 23.5 eV pass energy and the binding energy was corrected by contaminant carbon (C_{1s} = 285.0 eV). Peak fitting was done using XPSPEAK 4.1 with Shirley background and 30:70 Lorentzian/Gaussian convolution product shapes.

2.3. PROX Reaction

The PROX reaction was carried out in a fixed-bed glass reactor. 0.1 g catalyst was loaded in the reactor. The reactant gas containing 1.33% CO, 1.33% O_2, 65.33% H_2 and He for balance (vol. %) was fed into the reactor with a total flow rate of 50 ml/min. The ratio $[O_2]/[CO]$ was fixed at 1 in this study for a better comparison of the activity and selectivity among catalysts. The reactor was heated in a furnace with a heating rate of 2˚C/min. After reaching the reaction temperature for 5 min, the product was analyzed by a gas chromatograph equipped with a thermal conductivity detector using MS-5A packed column. CO conversion and selectivity of oxygen reacting with CO were calculated by the following equations:

$$\text{CO conversion } (X_{\text{CO}}\%) = \frac{[\text{CO}]_{\text{in}} - [\text{CO}]_{\text{out}}}{[\text{O}]_{\text{in}}} * 100\% \quad (3)$$

$$\text{O}_2 \text{ conversion } (X_{\text{O2}}\%) = \frac{[\text{O}_2]_{\text{in}} - [\text{O}_2]_{\text{out}}}{[\text{O}_2]_{\text{in}}} * 100\% \quad (4)$$

$$\text{Selectivity } (S\%) = \text{mol of } \text{O}_2 \text{ reacting with CO/mol of } \text{O}_2 \text{ consumed}$$

$$= \frac{0.5 * X_{\text{CO}}}{X_{\text{O}_2}} * 100\% \quad (5)$$

In all experiments, the carbon imbalance did not exceed ±1%.

3. Results and Discussion

3.1. ICP-MS

Table 1 shows the amount of Au loading on the catalyst. The isoelectric point of support would influence the Au loading and the particle size of Au. After adding $Mg(OH)_2$ in CeO_2, the isoelectric point of support increased. In this study, the pH value during DP process was fixed at 7, therefore the amount of Au loading increased after adding $Mg(OH)_2$. The results are in accord [1] [10].

3.2. BET Surface Area

The BET surface areas of Au/$Mg(OH)_2$-CeO_2 catalysts are listed in **Table 2**. It shows that the addition of $Mg(OH)_2$ in Au/CeO_2 increased the BET surface area of the catalyst. Since CeO_2 was crystalline phase, it had low surface area. $Mg(OH)_2$ was in amorphous phase and had higher surface area. Adding $Mg(OH)_2$ in CeO_2 increased the BET surface area of the catalyst, as expected.

3.3. XRD

In the XRD pattern of catalysts with different magnesium contents (**Figures 1(b)-(e)**), the characteristic peaks of CeO_2 at 2θ = 28.549˚ (111), 33.077˚ (200), 47.483˚ (220) were detected in all catalysts. However, the peaks of Au, which should present at 2θ = 38.184 (111), 44.392 (200) and 77.547 (311), were not detected in the XRD patterns, indicating that the particle size of gold particles were smaller than 5 nm [12] [13] [14] [15]. The results are consistent with the TEM results, which will be reported in the later section.

Table 1. Real Au loading on the catalyst (the nominal Au loading was 1 wt%).

Catalyst	Au loading (wt %)
Au/CeO_2	0.67
Au/$Mg(OH)_2$-CeO_2 (6.5%)	0.88
Au/$Mg(OH)_2$-CeO_2 (20%)	0.93
Au/$Mg(OH)_2$-CeO_2 (37.5%)	0.98
Au/$Mg(OH)_2$-CeO_2 (50%)	1.0

Table 2. BET surface areas of Au/$Mg(OH)_2$-CeO_2 catalysts.

Catalyst	BET surface area (m^2/g)
Au/CeO_2	69
Au/$Mg(OH)_2$-CeO_2 (6.5%)	114
Au/$Mg(OH)_2$-CeO_2 (20)	95
Au/$Mg(OH)_2$-CeO_2 (37.5%)	86
Au/$Mg(OH)_2$-CeO_2 (50)	84

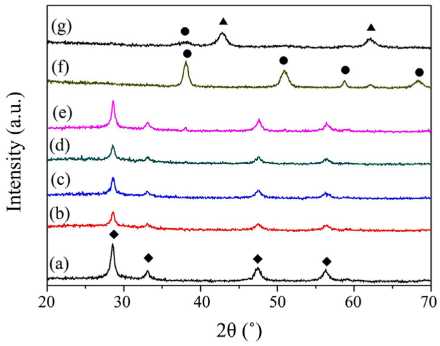

Figure 1. XRD pattern of Au/CeO_2 (a) and Au/$Mg(OH)_2$-CeO_2 catalyst with Mg/(Mg + Ce) = 6.5% (b), 20% (c), 37.5% (d), 50% (e). Au/$Mg(OH)_2$ (f) and MgO support (g).

It should be noted that the pure MgO support calcined at 380˚C existed in phase of both MgO ($2\theta = 42.917$ (200), 62.304 (220)) and $Mg(OH)_2$ ($2\theta = 38.016$ (101), 50.854 (102), 58.640 (110)), as shown in **Figure 1(g)**. After loading with gold, only $Mg(OH)_2$ phase was detected. $Mg(OH)_2$ was formed by reaction with water during depeosition-precipitation (DP) process:

$$MgO + H_2O \rightarrow Mg(OH)_2 \tag{6}$$

$Mg(OH)_2$ can be converted to MgO as the temperature was higher than 400˚C. Since the calcination temperature of the sample was 180˚C, Mg would be in the form of $Mg(OH)_2$. There was no significant difference in particle size of cerium oxide with different Mg contents.

The characteristic peaks of $Mg(OH)_2$ were not observed in the XRD patterns for all of the catalysts, excepted the one with Mg/(Mg + Ce) ratio of 50%. This indicates that $Mg(OH)_2$ was highly dispersed on CeO_2 surface. MgO phase was not observed in all samples. It was only detected in the Au/MgO sample.

3.4. TEM

As shown in the TEM photos in **Figure 2**, the gold particles were observed as small dark spots. The gray bulk mass was ceria support, while $Mg(OH)_2$ was surrounded on ceria with a lighter color. It shows that $Mg(OH)_2$ was on the surface of CeO_2 as a thin layer when the content of $Mg(OH)_2$ was low. Au was deposited on either CeO_2 or $Mg(OH)_2$ depending on the content of $Mg(OH)_2$. The average particles diameters of Au in these Au/$Mg(OH)_2$-CeO_2 with different Mg contents are listed in **Table 3**. The average size of Au on these catalysts was between 3.5 nm and 5 nm, the Au particle size decreased as the content of Mg increased.

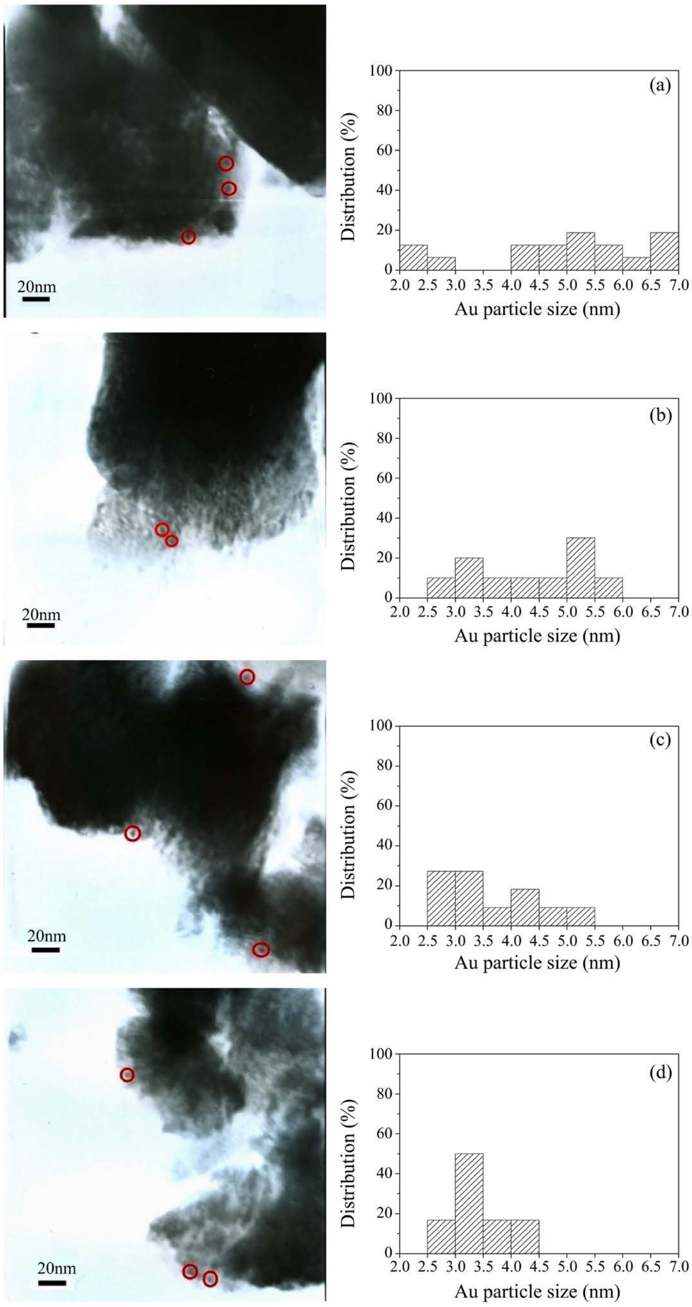

Figure 2. TEM images and Au particle diameter distributions of Au/$Mg(OH)_2$-CeO_2 catalysts with Mg/(Mg + Ce) ratio = (a) 6.5%, (b) 20%, (c) 37.5%, (d) 50%.

Table 3. Average particle diameter of Au nanoparticles in Au/$Mg(OH)_2$-CeO_2 catalysts.

Mg/(Mg + Ce) ratio	6.5%	20%	37.5%	50%
$d_{Au,ave}$ (nm)	4.9774	4.3059	3.7300	3.4461

3.5. HR-TEM

The HR-TEM image of Au/$Mg(OH)_2$-CeO_2 (20%) catalyst are shown in **Figure 3**. The d-spacing of 0.3063 nm is corresponded to CeO_2 (111) with standard d-spacing of 0.3124 nm. The d-spacing of 0.2351 nm is corresponded to $Mg(OH)_2$ (101) with standard d-spacing of 0.2365 nm. Gold with d-spacing 0.2335 nm (the standard d-spacing is 0.2355 nm) attached on the support was seen as well.

3.6. XPS

In the XPS analysis of Mg 2p, the binding energy of MgO is 50.8 eV and $Mg(OH)_2$ is 49.5 eV. The XPS Mg 2p spectra of this series of Au/$Mg(OH)_2$-CeO_2 catalyst are shown in **Figure 4**. The binding energies of Mg 2p peaks in all samples are tabulated in **Table 4**. The binding energies of Mg 2p of Au/$Mg(OH)_2$-CeO_2 catalysts are around 49.3 eV, indicating that the magnesium species were mainly existed as $Mg(OH)_2$, in agreement with the XRD results. The Mg/(Mg + Ce) ratios on the surface, obtained by XPS analysis, are listed in **Table 4**. As the nominal content of magnesium reached 37.5%, significant accumulation of Mg on the surface were observed.

XPS spectra of O 1s were applied to analyze the contents of various oxygen species on the surface (**Figure 5**). The O 1s spectra were separated into two peaks: lattice oxygen at 529 eV and hydroxide species at 531 eV. The lattice oxygen was attributed to the oxygen existed in the lattice of CeO_2 while the hydroxide species assigned to the $Mg(OH)_2$ species. Among all of the Au/$Mg(OH)_2$-CeO_2 catalysts, the one with 6.5% of Mg/(Mg + Ce) ratio had the highest amount of hydroxide species compared to the others (**Table 5**).

The XPS spectra of Au 4f are shown in **Figure 6**, and the concentrations of various electronic states of Au on $Mg(OH)_2$-CeO_2 with different Mg/(Mg + Ce) atomic ratios are listed in **Table 6**. Gold displayed two peaks of Au $4f_{7/2}$ and Au $4f_{5/2}$ at around 84 eV and 88 eV. The peak of Mg 2s at 89 eV overlapped with Au $4f_{5/2}$. The metallic gold and oxidic gold displayed peaks at 87.57 eV and 88.2 eV in Au $4f_{5/2}$, and at 83.9 eV and 84.7 eV in Au $4f_{7/2}$ [1] [2] [3] [4] [5]. **Table 6** shows that the higher concentration of metallic gold species was observed with higher content of $Mg(OH)_2$ in the catalyst. In the samples with low content of $Mg(OH)_2$, most of Au was deposited on CeO_2. Au would have strong interaction with CeO_2. Since CeO_2 has more defect sites, it would cause Au in electron-deficient. In the samples with high concentration of $Mg(OH)_2$, most of Au would deposit on the surface of $Mg(OH)_2$, resulting in metallic gold species.

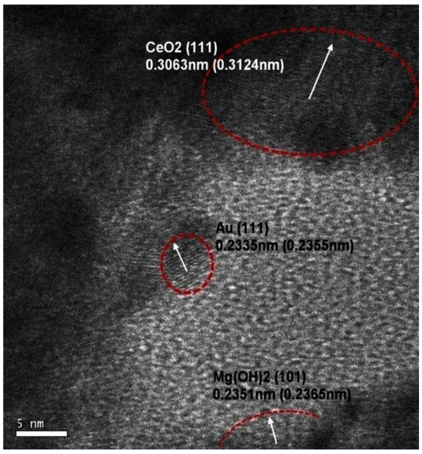

Figure 3. HR-TEM image of Au/$Mg(OH)_2$-CeO_2 with Mg/(Mg + Ce) = 10%.

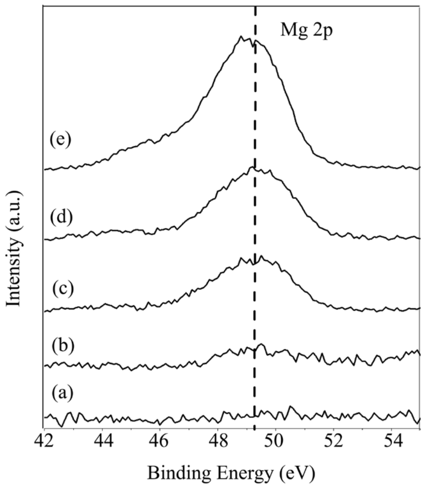

Figure 4. XPS Mg 2p spectra of Au/$Mg(OH)_2$-CeO_2 catalysts with Mg/(Mg + Ce) = 6.5% (a), 20% (b), 37.5% (c), 50% (d), and Au/$Mg(OH)_2$ (e).

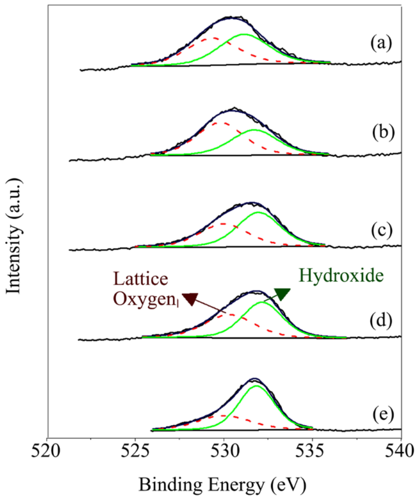

Figure 5. XPS O 1s spectra of Au/$Mg(OH)_2$-CeO_2 catalysts with Mg/(Mg + Ce) = 6.5% (a), 20% (b), 37.5% (c), 50% (d), and Au/$Mg(OH)_2$ (e).

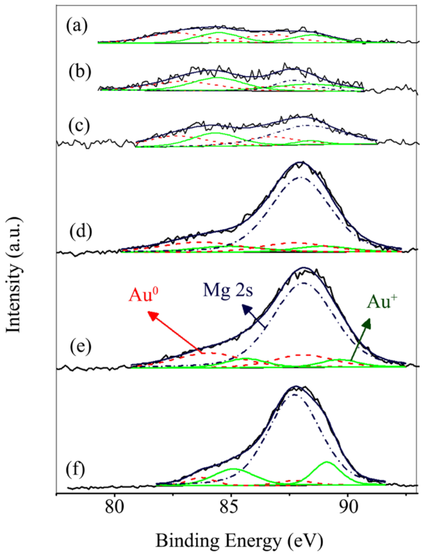

Figure 6. XPS Au 4f spectra of Au/CeO$_2$ (a), Au/Mg(OH)$_2$-CeO$_2$ catalysts with Mg/(Mg + Ce) = 6.5% (b), 20% (c), 37.5% (d), 50% (e) and Au/Mg(OH)$_2$ (f).

Table 4. Mg 2p XPS analysis of Au/Mg(OH)$_2$-CeO$_2$ catalysts.

Catalyst	peak position of Mg 2p (eV)	Mg/(Mg + Ce) ratio on surface (%)
Au/Mg(OH)$_2$-CeO$_2$ (6.5%)	49.44	5.76
Au/Mg(OH)$_2$-CeO$_2$ (20%)	49.46	11.55
Au/Mg(OH)$_2$-CeO$_2$ (37.5%)	49.55	63.53
Au/Mg(OH)$_2$-CeO$_2$ (50%)	49.29	76.10
Au/Mg(OH)$_2$	48.91	100

Table 5. O 1s XPS analysis of Au/Mg(OH)$_2$-CeO$_2$ catalysts with different Mg contents.

Catalyst	peak position of O 1s (eV)	Surface content of O	
		Lattice oxygen (%)	Hydroxyl (%)
Au/Mg(OH)$_2$-CeO$_2$ (6.5%) *	530.44	44.02	55.98
Au/Mg(OH)$_2$-CeO$_2$ (20%)	530.58	48.70	51.30
Au/Mg(OH)$_2$-CeO$_2$ (37.5%)	531.33	56.76	43.23
Au/Mg(OH)$_2$-CeO$_2$ (50%)	531.45	50.54	49.46
Au/Mg(OH)$_2$	531.51	33.34	66.66

*Mg/(Mg + Ce) in catalyst.

Table 6. Au 4f XPS analysis of Au/Mg(OH)$_2$-CeO$_2$ catalysts with different Mg contents.

Catalyst	Surface content of Au	
	Au^0 (%)	Au = (%)
Au/Mg(OH)$_2$-CeO$_2$ (6.5%)	41.54	58.46
Au/Mg(OH)$_2$-CeO$_2$ (20%)	59.40	40.60
Au/Mg(OH)$_2$-CeO$_2$ (37.5%)	65.60	34.40
Au/Mg(OH)$_2$-CeO$_2$ (50%)	72.37	27.63
Au/Mg(OH)$_2$	72.38	27.62

3.7. PROX Reaction

Figure 7 and **Figure 8** show the effect of Mg content on the performance of PROX over Au/$Mg(OH)_2$-CeO_2 catalysts. CO conversion increased with increasing temperature until 40˚C or 60˚C, depending on sample, and then level off. At high temperature, H_2 would compete with CO to react with O_2, and resulted in low CO selectivity. At lower reaction temperature, the existence of magnesium did not facilitate the CO conversion; instead, lower CO conversion was observed, except the sample with Mg/(Mg + Ce) ratios of 6.5%. **Figure 8** shows that the samples modified with $Mg(OH)_2$ had high selectivity of CO oxidation at low reaction temperature, indicating that the presence of $Mg(OH)_2$ could suppress H_2 oxidation. Au/$Mg(OH)_2$-CeO_2 catalysts showed higher CO oxidation selectivity than the unmodified Au/CeO_2 catalyst at any reaction temperature. All catalysts had high CO conversion at temperature 80˚C - 100˚C. Nevertheless, the Au/$Mg(OH)_2$-CeO_2 still had a higher CO conversion, although the difference was very small, since Au/CeO_2 already has conversion reaching 99%. The Au/$Mg(OH)_2$-CeO_2 (20%) catalyst was run at 80˚C for 120 h time on stream, it did not show any decay, indicating this catalyst was very stable.

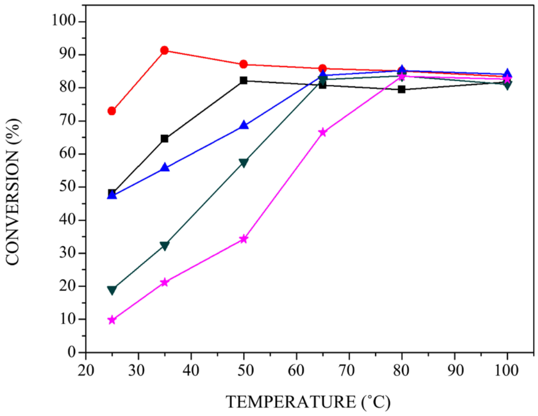

Figure 7. CO conversions of Au/CeO_2 (■) and Au/$Mg(OH)_2$-CeO_2 with different Mg/(Mg + Ce) ratios: 6.5% (●), 20% (▲), 37.5% (▼), 50% (★).

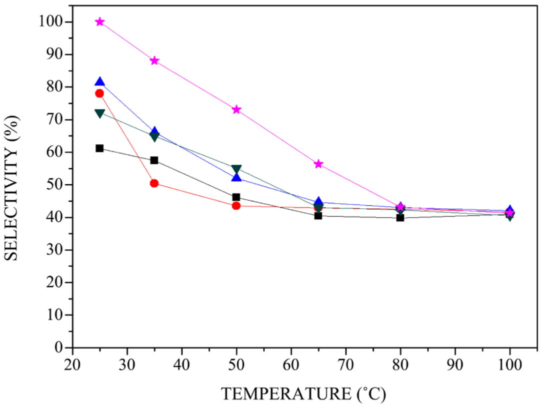

Figure 8. CO selectivity of Au/CeO_2 (■) and Au/$Mg(OH)_2$-CeO_2 with different Mg/(Mg + Ce) ratios: 6.5% (●), 20% (▲), 37.5% (▼), 50% (★).

$Au/Mg(OH)_2$-CeO_2 (20%) catalyst showed the highest activity among all catalysts, it also possessed the highest ratio of hydroxyl species. This confirms that the OH species between the interface of gold and support is the species to activate CO oxidation reaction. Molina and Hammer [19] reported that the Au-Au coordination determined the local reactivity of the Au atoms and the presence of the MgO support that, besides providing excess electrons to the Au clusters, forms ionic bonds to the peroxo part of the CO-O_2 reaction intermediate. They [19] reported that the type of interface boundary likely to be predominant for medium-sized nanoparticles provides the optimal degree of low-coordinated Au atoms in the neighborhood of the MgO support. Our results are in accord.

The metallic gold was believed to be the active site for PROX reaction [20]-[28]. The amount of Au^0 in the catalysts increased with the increase of magnesium content as shown in **Table 5**. However, overdoes of $Mg(OH)_2$ would retard the CO adsorption and suppress CO oxidation. It also suppressed H_2 oxidation and thus there was enough O_2 to react with CO [13] [21]. The results clearly demonstrate that adding $Mg(OH)_2$ in Au/CeO_2 could suppress H_2 oxidation and therefore increase CO oxidation activity.

4. Conclusion

A series of $Au/Mg(OH)_2$-CeO_2 catalysts were prepared. $Mg(OH)_2$ would form a thin layer on the surface of CeO_2. CeO_2 was in the crystalline phase and $Mg(OH)_2$ was amorphous. Using CeO_2 as a support could increase the dispersion of $Mg(OH)_2$ and thus increase the interaction between Au and $Mg(OH)_2$. The amount of Au^0 in the catalysts increased with the increase of magnesium content. However, overdoes of $Mg(OH)_2$ would retard the CO adsorption and suppress CO oxidation. It also suppressed H_2 oxidation, and thus there was enough O_2 to react with CO. The results clearly demonstrate that adding $Mg(OH)_2$ in Au/CeO_2 could suppress H_2 oxidation and therefore increase CO oxidation activity.

Acknowledgements

This research was supported by the Ministry of Science and Technology, Taiwan.

Conflicts of Interest

The authors declare no conflicts of interest regarding the publication of this paper.

References

[1] Chen, Y.W. and Sasirekha, N.S. (2014) Preferential Oxidation of CO in H_2 Stream over Gold Catalysts. In: Ma, Z. and Dai, S., Eds., *Heterogeneous Gold Catalysts and Catalysis*, Royal Society of Chemistry, Cambridge, RSC Catalysis Series, No. 18, 73-103.

[2] Maciel, C.G., Silva, T.F., Hirooka, M.I., Belgacem, M.N. and Assaf, J.M. (2012) Effect of Nature of Ceria Support in CuO/CeO_2 Catalyst for PROX-Co Reaction. *Fuel*, **97**, 245-252. https://doi.org/10.1016/j.fuel.2012.02.004

[3] Ayastuy, J.L., Gamboa, N.K., González-Marcos, M.P. and Gutiérrez-Ortiz, M.A.

(2011) CuO/CeO_2 Washcoated Ceramic Monoliths for CO-PROX Reaction. *Chemical Engineering Journal*, **171**, 224-231. https://doi.org/10.1016/j.cej.2011.03.006

[4] Yang, Y.F., Sangeetha, P. and Chen, Y.W. (2009) $Au/FeO_x\text{-}TiO_2$ Catalysts for the Preferential Oxidation of CO in H_2 Stream. *Industrial & Engineering Chemistry Research*, **48**, 10402-10407. https://doi.org/10.1021/ie900806r

[5] Sangeetha, P., Zhao, B. and Chen, Y.W. (2010) $Au/CuO_x\text{-}TiO_2$ Catalysts for Preferential Oxidation of CO in Hydrogen Stream. *Industrial & Engineering Chemistry Research*, **49**, 2096-2102. https://doi.org/10.1021/ie901233e

[6] Chen, Y.W., Chen, H.J. and Lee, D.S. (2012) $Au/Co_3O_4\text{-}TiO_2$ Catalysts for Preferential Oxidation of CO in H_2 Stream. *Journal of Molecular Catalysis A*: *Chemical*, **363-364**, 470-480. https://doi.org/10.1016/j.molcata.2012.07.027

[7] Chen, Y.W., Lee, D.S. and Chen, H.J. (2012) Preferential Oxidation of CO in H_2 Stream on $Au/ZnO\text{-}TiO_2$ Catalysts. *International Journal of Hydrogen Energy*, **37**, 15140-15155. https://doi.org/10.1016/j.ijhydene.2012.08.003

[8] Duh, F.C., Lee, D.S. and Chen, Y.W. (2013) $Au/CuO_x\text{-}TiO_2$ Catalysts for CO Oxidation at Low Temperature. *Modern Research in Catalysis*, **2**, 1-8. https://doi.org/10.4236/mrc.2013.21001

[9] Lee, D.S. and Chen, Y.W. (2013) Synthesis of $Au/CoO_x\text{-}TiO_2$ Catalysts and Its Application for Low Temperature CO Oxidation. *Journal of Catalysts*, **2013**, Article ID: 586364. https://doi.org/10.1155/2013/586364

[10] Sasirekha, N., Sangeetha, P. and Chen, Y.W. (2014) Bimetallic $Au\text{-}Ag/CeO_2$ Catalysts for Preferential Oxidation of CO in Hydrogen-Rich Stream: Effect of Calcination Temperature. *Journal of Physical Chemistry C*, **118**, 15226-15233. https://doi.org/10.1021/jp500102g

[11] Grisel, R.J.H. and Nieuwenhuys, B.E. (2001) Selective Oxidation of CO, over Supported Au Catalysts. *Journal of Catalysis*, **199**, 48-59. https://doi.org/10.1006/jcat.2000.3121

[12] Grisel, R.J.H., Slyconish, J.J. and Nieuwenhuys, B.E. (2001) Oxidation Reactions over Multi-Component Catalysts: Low-Temperature CO Oxidation and the Total Oxidation of CH_4. *Topics in Catalysis*, **16-17**, 425-431. https://doi.org/10.1023/A:1016694022941

[13] Grisel, R.J.H., Weststrate, C.J., Goossens, A., Crajé, M.W.J., van der Kraan, A.M. and Nieuwenhuys, B.E. (2002) Oxidation of CO over $Au/MO_x/Al_2O_3$ Multi-Component Catalysts in a Hydrogen-Rich Environment. *Catalysis Today*, **72**, 123-132. https://doi.org/10.1016/S0920-5861(01)00486-2

[14] Tompos, A., Hegedus, M., Margitfalvi, J.L., Szabo, E.G. and Vegvari, L. (2008) Multicomponent Au/MgO Catalysts Designed for Selective Oxidation of Carbon Monoxide: Application of a Combinatorial Approach. *Applied Catalysis A*: *General*, **334**, 348-356. https://doi.org/10.1016/j.apcata.2007.10.022

[15] Yang, Z., Wu, R., Zhang, Q. and Goodman, D.W. (2002) Adsorption of Au on an O-Deficient MgO(001) Surface. *Physical Review B*, **65**, 155407-155411. https://doi.org/10.1103/PhysRevB.65.155407

[16] Tyo1, E.C. and Vajda, S. (2015) Catalysis by Clusters with Precise Numbers of Atoms. *Nature Nanotechnology*, **10**, 577-588. https://doi.org/10.1038/nnano.2015.140

[17] Wang, Z., Xu, C. and Wang, H. (2014) A Facile Preparation of Highly Active Au/MgO Catalysts for Aerobic Oxidation of Benzyl Alcohol. *Catalysis Letters*, **144**, 1919-1925. https://doi.org/10.1007/s10562-014-1344-z

[18] Chang, L.H., Chen, Y.W. and Sasirekha, N. (2008) Preferential Oxidation of Carbon Monoxide in Hydrogen Stream over Au/MgO_x-TiO_2 Catalysts. *Industrial & Engineering Chemistry Research*, **47**, 4098-4105. https://doi.org/10.1021/ie071590d

[19] Molina, L.M. and Hammer, B. (2004) Theoretical Study of CO Oxidation on Au Nanoparticles Supported by MgO(100). *Physical Review B*, **69**, 155424-155445. https://doi.org/10.1103/PhysRevB.69.155424

[20] Haruta, M. (2004) Nanoparticulate Gold Catalysts for Low-Temperature CO Oxidation. *Journal of New Materials for Electrochemical Systems*, **7**, 163-172. https://doi.org/10.1002/chin.200448226

[21] Min, B.K. and Friend, M. (2007) Heterogeneous Gold-Based Catalysis for Green Chemistry: Low-Temperature CO Oxidation and Propene Oxidation. *Chemical Reviews*, **107**, 2709-2724. https://doi.org/10.1021/cr050954d

[22] Thompson, D.T. (2007) Using Gold Nanoparticles for Catalysis. *Topics in Catalysis*, **44**, 331. https://doi.org/10.1007/s11244-007-0307-7

[23] Chen, M. and Goodman, D.W. (2008) Promotional Effects of Au in Pd-Au Catalysts for Vinyl Acetate Synthesis. *Chinese Journal of Catalysis*, **29**, 1178-1186. https://doi.org/10.1016/S1872-2067(09)60021-8

[24] Chan, S.C. and Barteau, M.A. (2005) Preparation of Highly Uniform Ag/TiO_2 and Au/TiO_2 Supported Nanoparticle Catalysts by Photodeposition. *Langmuir*, **21**, 5588-5595. https://doi.org/10.1021/la046887k

[25] Date, M., Ichihashi, Y., Yamashita, T., Chiorino, A., Boccuzzi, F. and Haruta, M. (2002) Performance of Au/TiO_2 Catalyst under Ambient Conditions. *Catalysis Today*, **72**, 89-94. https://doi.org/10.1016/S0920-5861(01)00481-3

[26] Pattrick, G.E., van der Lingen, C.W., Corti, R.J., Holliday, H. and Thompson, D.T. (2004) The Potential for Use of Gold in Automotive Pollution Control Technologies: A Short Review. *Topics in Catalysis*, **30**, 273-279. https://doi.org/10.1023/B:TOCA.0000029762.14168.d8

[27] Hartadi, Y., Behm, R.J. and Widmann, D. (2016) Competition of CO and H_2 for Active Oxygen Species during the Preferential CO Oxidation (PROX) on Au/TiO_2 Catalysts. *Catalysts*, **6**, 21-34. https://doi.org/10.3390/catal6020021

[28] Lin, X., Yang, B., Benia, H.M., Myrach, P., Yulikov, M., Aumer, A., Brown, M.A., Sterrer, M., Bondarchuk, O., Kieseritzky, E., Rocker, J., Risse, T., Gao, H.J., Nilius, N. and Freund, H.J. (2010) Charge-Mediated Adsorption Behavior of CO on MgO-Supported Au Clusters. *Journal of the American Chemical Society*, **132**, 7745-7754. https://doi.org/10.1021/ja101188x